

# **Chapter 1**

## **Introduction and Inspirations of thesis**

*“Chapter 1 gives a brief overview of the phenomena of luminescence, its types, photoluminescence mechanism, phosphor materials, and the characteristics of rare-earth elements. The limits and difficulties of phosphors used in industrial wLED and its dependent parameters are covered in this chapter. The structural and luminescent characteristics of the  $\text{CaMoO}_4$  phosphor employed in the thesis work are also specifically examined in this chapter. At the end of this chapter, the thesis's rationale is described. It is based on research of numerous phosphors utilized in various optoelectronic applications.”*



### **1.1 Historical background of luminescence**

The phenomena of Luminescence (such as glowing fungi, glowing insects, rotting wood, colorful aurora, etc.) have fascinated and curious mankind since the earliest times. The first scientific mention of the luminescence phenomenon was published in 1852 by the English physicist Sir G. G. Stokes in the article "On the refrangibility of light" and gave Stokes' law to understand the luminescence phenomenon.<sup>1</sup> This law states that the emission wavelength of a luminescent compound or organism is greater than its excitation. Subsequently, in 1888, the German physicist and historian Eilhard Wiedemann used luminescence term to refer to all light-emitting phenomena that were different from the light produced by an increase in temperature.<sup>2</sup> The Lumen term in Luminescence is from the Latin language which means light. Hence, luminescence is the visible radiation that is emitted from specific materials or organisms as a result of mechanical pressure, chemical reactions, physiological processes, radioactive radiation, electrical energy, piezoelectricity or subatomic motion. Luminescence is completely different from the incandescence phenomenon because the luminescence phenomenon is the release of already absorbed radiation upon heating whereas the incandescent phenomenon is the emission of visible light by a heated material. Therefore, due to these different types of excitation, the luminescence phenomenon has been classified into several parts.

### **1.2 Types of Luminescence**

The luminescence phenomena may be categorized into 6 categories which are based on the type of stimulation, as discussed below and shown in Fig. 1.1.

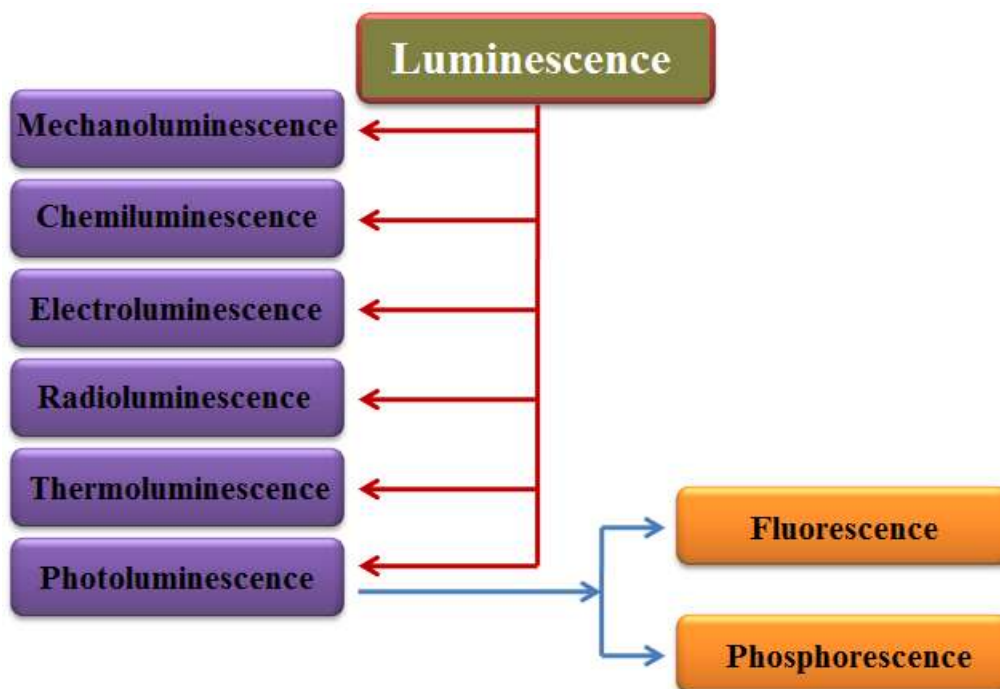


Fig. 1.1 Types of luminescence depend on modes of excitation and time duration.

### 1.2.1 Mechanoluminescence (ML)

The phenomenon of radiation produced by mechanical action on a solid is called mechanoluminescence (ML). These mechanical actions are mainly cutting, rubbing, moving, grinding, scratching, or compression. The ML can also be excited by thermal shocks caused by a sample being severely cooled or heated, or by shock waves produced when a sample is exposed to powerful laser pulses. The ML may also be seen during the separation of two distinct materials that are in contact with the deformations brought about by phase transitions or crystal development. The ML process may also go by the labels sonoluminescence, fractoluminescence, triboluminescence, or piezoluminescence depending on the kind of mechanical force that is delivered to the solid.

### **1.2.2 Chemiluminescence (CL)**

Chemiluminescence (CL) is the phenomenon in which emitted electromagnetic radiation due to specific chemical processes that result in excited molecules emitting a large amount of energy in the form of photons when they relax in the ground state. The CL process is widely used in the applications of clinical analysis. Bioluminescence is one form of CL, which is produced by biological processes within a living thing. Less than 20% of light in bioluminescence causes heat. In light of this, bioluminescence is also known as cold light. Fireflies and sea invertebrates are only two examples of the numerous bioluminescent species.

### **1.2.3 Electroluminescence (EL)**

In this phenomenon, the generation of photons is emitted due to the flow of electric current in the material. These photons are emitted as a result of the recombination of electrons and holes in the depletion region of the P-N junction semiconductor. This phenomenon of luminescence is called electroluminescence (EL). EL phenomenon is widely used in optoelectronic devices such as electroluminescent displays, LEDs, etc.

### **1.2.4 Radioluminescence (RL)**

The EM radiation is emitted due to the excitation of matter by ionizing particles (such as  $\alpha$  particles,  $\beta$  particles, or  $\gamma$  rays) in the radio luminescence (RL) process. Therefore, ionizing particles are the source of excitation in radio luminescence. The substances which show this phenomenon is called scintillators. The Tritium-excited luminous paints used on watch dials are a common example of the RL phenomenon. In these, the luminous paints are excited by very low-energy  $\beta$  radiation emanating from the tritium nucleus.

### **1.2.5 Thermoluminescence (TL)**

The thermoluminescence (TL) process uses heat as the excitation source of thermally stimulated luminescence. In some crystalline materials, electrons are already trapped in the defect state which occurs due to distortion in the crystal structure. When these substances receive the required thermal energy they release trapped electrons, resulting in EM radiation, a process known as thermoluminescence (TL). The latent energy required to release the trapped electrons is estimated by the emission curves. The TL process is used for radiation dosimeter and archaeological materials dating.

### **1.2.6 Photoluminescence (PL)**

This phenomenon of luminescence involves photons as a source of excitation. The molecules are excited by the incident photon, and then the excited molecules return from the excited equilibrium state to the ground state and result in the emission of EM radiations. This process of luminescence is called photoluminescence (PL). PL spectroscopy determines the electronic structure, optical properties and photochemical properties of samples, as well as information about interfacial point defects in samples. There are many applications based on PL in the field of optoelectronics such as fluorescent display devices, fluorescent lamps, fluorescence microscopy and spectroscopy, detection of hidden fingerprints, detection of counterfeit currency, remote sensing, UV sensing, security devices, lighting devices and optical Thermometry, etc. Based on the lifetime of the emission process, PL is classified into two parts, which are fluorescence and phosphorescence, respectively.

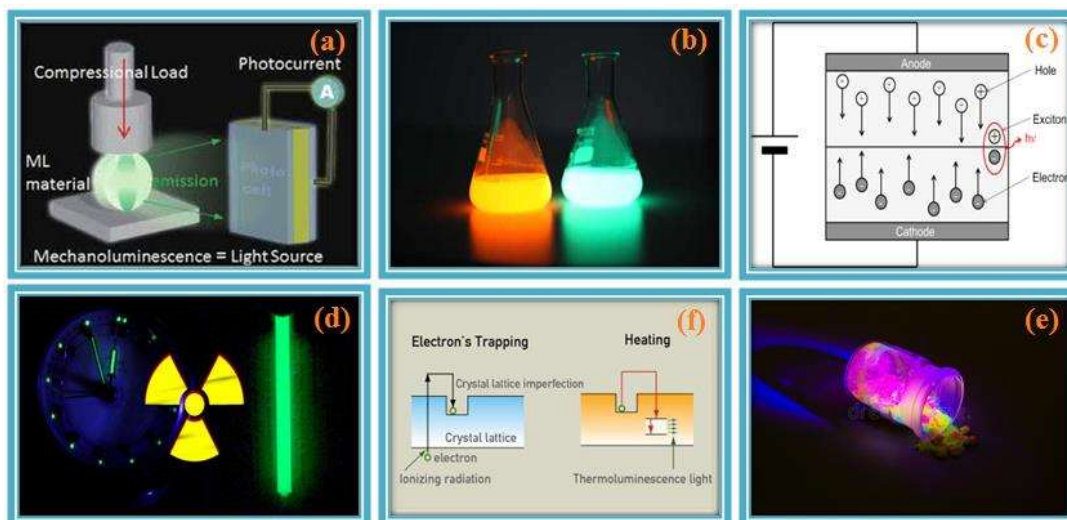


**Fig. 1.2** (a) Mechanoluminescence process, (b) Chemiluminescence in a chemical solution, (c) Electroluminescence process, (d) Tritium-based watch dial (radioluminescence), (e) Thermoluminescence process, (f) Photoluminescence phenomenon.

Fluorescence is described as a light emission that decreases with the end of excitation while phosphorescence is the opposite which is described as the emission of light beyond the end of excitation. However, due to the existence of both short-lived phosphorescence and long-lived fluorescence, which have the same duration, this line of thinking is insufficient to understand both phenomena. Therefore, we need to know the differences between both processes in detail, which are explained below respectively.

### 1.2.6.1 Fluorescence

Fluorescence is a type of photoluminescence in which a molecule is excited from the singlet ground state to an excited singlet state by absorbing high-energy photons and then relaxes to the excited equilibrium state by non-radiative transitions. Thereafter, it returns from the excited state to the ground singlet state and emits a photon with lower energy than the absorbed photon. The required time for the fluorescence process is  $10^{-4}$  to  $10^{-8}$  seconds. In this process, the spin multiplicity remains constant, so there is no change or disturbance in the spin of the electrons. Many living biological forms show photoluminescence due to

fluorescence phenomena such as the fluorescent pumpkin in the Atlantic forest of Brazil. The applications of the fluorescence phenomenon are mainly in fluorescent lamps, paints, dyes and biological markers etc.

### **1.2.6.2 Phosphorescence**

Phosphorescence is the process of photoluminescence in which the spin of an electron is not constant but is reversed. In this phenomenon, the excited molecule in the excited singlet state moves to an intermediate excited triplet state by intersystem crossing due to molecular collisions. The singlet to triplet transition occurs due to the reversal of electron spin. After that, EM radiation is emitted when the molecule comes from the excited triplet state to the ground singlet state, called the phosphorescence phenomenon. Whereas the transition from the triplet state to the singlet state is more improbable than the transition from the singlet state to the singlet state because of the difference in spin orientation between the excited triplet state and the ground singlet state, resulting in significantly longer emission lifetimes ( $\sim 10^{-3}$  s to 100 s). Hence, this phenomenon is also called delayed fluorescence. Thus, the phenomenon of displaying a glow for a long time on incident light in a material is called phosphorescence.

### **1.3 PL process mechanism**

The substances showing the phenomenon of luminescence are called phosphor materials. Usually, the phosphor material is formed by the impurity doping into a suitable host crystal; these impurities are called activator ions or luminescence centers. The molecule gets excited by absorbing the incident photon's energy after which it emits radiation due to its relaxation. These emissions may be due to the host matrix as well as to the doped ions. The electronic transition of the doped ions that results in the emission of radiation is called activator ions. If the absorption of the activator ion is weak, other ions are co-doped in the

host matrix and are called sensitizers. Thus the incident energy is well absorbed by the activator ions, thereby improving the emission of photons.<sup>2</sup> All processes taking place in the phosphor material are shown in the Jablonski diagram.

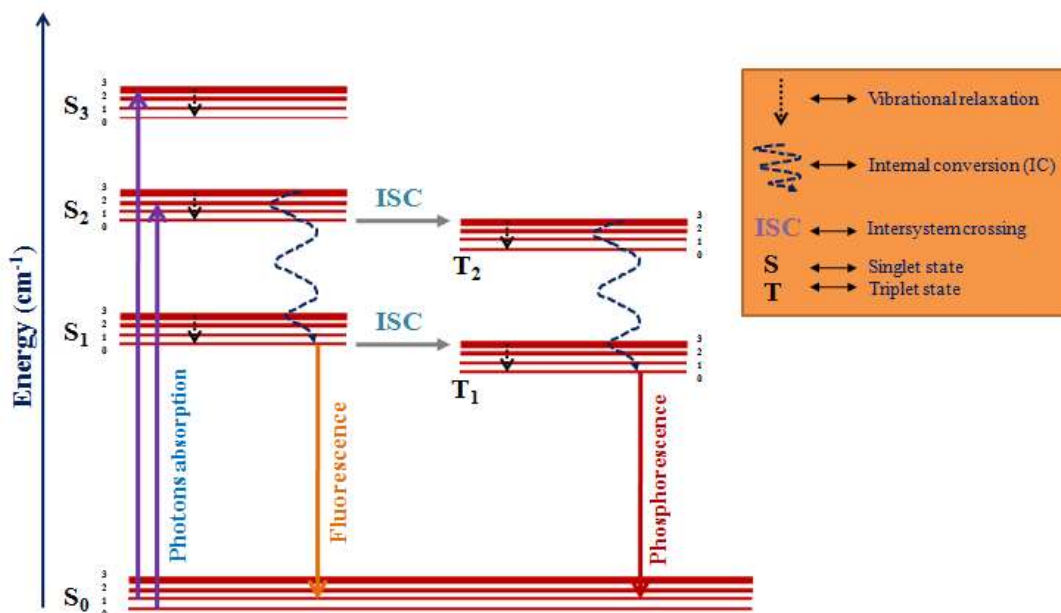


**Fig. 1.3** Jablonski diagram for explaining the Fluorescence and Phosphorescence phenomenon.

The Jablonski diagram was designed by Professor Alexander Jablonski and is mainly used to understand fluorescence spectroscopy. Fig. 1.3 shows a typical Jablonski diagram in which S<sub>0</sub>, S<sub>1</sub>, S<sub>2</sub>, and S<sub>3</sub> are singlet ground states and sequentially singlet excited states, respectively. Furthermore, T<sub>1</sub> and T<sub>2</sub> are triplet excited states, respectively. The vibrational energy levels have been marked from 0, 1, 2, and 3 in each state. Generally, the emission energy is smaller than the absorption energy, which is called Stokes' law. All the processes involved in the phosphor material are described as follows;

### 1.3.1 Excitation process

The excitation electronic transition occurs as a result of the energy of the incident photon being absorbed by the molecule. The excitation spectrum of the sample in the range of

wavelength is analyzed by monitoring the wavelength of the maximum intensity emission. The excitation energy transfers the molecule, which moves from the ground singlet state to a higher vibration level in the excited singlet state. Phosphor materials show luminescence by absorbing EM radiation in the form of excitation energy. The absorption energy for the activator ions occurs through the host lattice. If the host absorbs energy, it may be that the received emission is by the host, or energy transfer from the host to the activator ions may be followed by the emission of the activator ions. Most often, high-energy ultraviolet (UV) radiation is used for excitation, which results in the emission of near-UV and visible radiation. In cases where the absorption of activator ions is weak, sensitizers are co-doped into the host lattice, which provides to help of excitation of activator ions. The excitation phenomenon of phosphor material is an instantaneous process that takes nearly a few femto seconds.

### **1.3.2 Emission process**

The transition of a molecule from an excited state to a ground state is a spontaneous process. Photoluminescence includes both non-radiative and radiative transition processes. The excited molecule releases energy through non-radiative emissions such as vibrational relaxation, internal conversion and intersystem crossing, and radiative emissions such as fluorescence and phosphorescence.

#### **1.3.2.1 Non-radiative emission**

The excited state of the molecule reaches a higher vibrational state after absorbing high-energy photons. When excited electrons return directly to the ground state without emitting photons, the transition is called non-radiative emission. In this process, the excited electrons transfer their energy to the lattice vibrations of the host, which directly emit energy in the form of phonons. Photoluminescence includes several types of non-radiative relaxation

such as vibrational relaxation, internal conversion (IC), and intersystem crossing (ISC). The non-radiative transition between vibrational levels of an excited state is called vibrational relaxation. When a non-radiative relaxation occurs between exciting levels of the same spin multiplicity, it is called internal conversion (IC), the  $S_2$  to  $S_1$  transition shown in Fig. 1.3 is an example of an IC. This transition is spin-allowed, leading to a rapid transition that takes  $10^{-12}$  seconds or less. Intersystem crossings (ISC) are non-radiative transitions in excited states with different spin multiplicities. The transition from the excited singlet state to the excited triplet state is the ISC process as shown in Fig. 1.3. The ISC is spin-prohibited, which results in a longer transition time than the IC, which is in the range of  $10^{-8}$  to  $10^{-3}$  seconds.

### 1.3.2.2 Radiative emission

The electromagnetic radiation obtained when the activator ions undergo an electronic transition from an excited state to a ground state is called a radiative transition. The radiative emission is obtained from an electronic transition from an excited singlet state to a ground singlet state and an excited triplet state to a ground singlet state. In Fig. 1.3, the  $S_1 \rightarrow S_0$  shown is a singlet to singlet radiation transition resulting in fluorescence, and  $T_1 \rightarrow S_0$  is a singlet to triplet radiation transition resulting in phosphorescence. Fluorescence emission consists of a spin-allowed transition; as a result, the process takes very less time ( $10^{-8}$  s). Whereas in phosphorescence the spin-prohibited transition occurs due to the variation in spin multiplicity, which makes the processing time more. The wavelength of the emitted radiation is greater than the wavelength of the absorbed radiation according to Stokes' law in both transitions. The radiative transition in the phosphor material is analyzed by the emission spectrum which is excited at the wavelength of maximum intensity of the excitation spectrum.

### **1.3.3 PL decay mechanism**

The lifetime of fluorescence is the average time a fluorophore is excited. To understand the lifetime of fluorescence, we imagine a sample consisting of several fluorophores. When we excite the sample with a high-energy electromagnetic pulse, some fluorophores get excited. Let us assume that the initial number of excited fluorophores is  $n_0$ . This excited population decreases continuously at a  $(A + B_{nr})$  rate whose equation is as follows<sup>3</sup>;

$$\frac{dn(t)}{dt} = -(A + B_{nr}) n(t) \quad 1.1$$

where  $n(t)$  is the population of excited fluorophores after  $t$  sec.  $A$  and  $B_{nr}$  are radiative emission rate and non-radiative emission rate, respectively. Emission is a random process, but each fluorophore has an equal probability of emission in a given time interval causing the population of the excited state to decrease exponentially;

$$n(t) = n_0 \exp\left(-\frac{t}{\tau}\right) \quad 1.2$$

The intensity of the emission received from the fluorescence spectrometer depends on the number of photons emitted. Hence, equation 1.2 can also be written in terms of intensity.

$$I(t) = I_0 \exp\left(-\frac{t}{\tau}\right) \quad 1.3$$

where  $I(t)$  and  $I_0$  are the intensity of emission in time  $t$  and intensity at time  $t = 0$ , respectively.  $\tau$  is decay fluorescence lifetime, which is equal to the inverse of the decay rate  $((A + B_{nr})^{-1})$ .<sup>3</sup> Thus, the slope of a plot  $\ln(I(t))$  versus  $t$  gives the information of the decay fluorescence lifetime.

Sometimes fluorophores decay in more than one way. For example, when two types of lanthanide ions (let's say  $\text{Ln}_1^{3+}$  and  $\text{Ln}_2^{3+}$ ) are present in a sample and energy transfer from

$\text{Ln}_1^{3+}$  to  $\text{Ln}_2^{3+}$  is also taking place, the  $\text{Ln}_1^{3+}$  ions decay into two electrons in two different ways. The first is when the excited electrons of  $\text{Ln}_1^{3+}$  will directly come to the ground state, and the second is when the excited electrons of  $\text{Ln}_1^{3+}$  after transferring to the excited state of  $\text{Ln}_2^{3+}$  will come to the ground state. Hence excited electrons of lanthanides ions can have two decay times whose intensity will follow a bi-exponential function after time  $t$ ,<sup>4</sup>

$$I(t) = I_0 + A_1 \exp\left(-\frac{t}{\tau_1}\right) + A_2 \exp\left(-\frac{t}{\tau_2}\right) \quad 1.4$$

where  $\tau_1$ ,  $\tau_2$  are fast and slow decay lifetimes, and  $A_1$ ,  $A_2$  are their corresponding amplitudes.

#### **1.4 Phosphor materials**

Luminescent substances that emit photons when excited by an external energy source such as incident high-energy photons are called phosphor materials. Phosphor is a Latin word that means 'bringing of light'. Phosphor materials are mainly composed by doping of activator ions in the host lattice. In general, the activator ion is that metal ion whose last orbital electron is in the 3d or 4f sub-shells, which are transition metal ions and rare-earth ions, respectively. The group of all the lanthanides, yttrium and scandium, are called rare-earth elements. There are two modes of luminescence observed in phosphor materials, first by the semiconductor host substance and second by the doped activator ions. In a host substance, luminescence occurs after band-to-band excitation between impurity levels formed in its bandgap, whereas luminescence due to activator ions results from emission into intermediate energy levels of the activator ion formed in the bandgap. The transition of excited electrons to intermediate energy levels of the activator ion can occur in two main ways, either from the excited level of the host or by the activator ion's self-excitation. For example, the 4f to 4f electronic transition of  $\text{Eu}^{3+}$  ion in  $\text{Eu}^{3+}$  doped  $\text{Gd}_2\text{O}_3$  phosphor.<sup>5</sup>

Generally, phosphates<sup>6</sup>, aluminates<sup>7</sup>, silicates<sup>8</sup>, oxides<sup>9</sup>, fluorides<sup>10</sup>, borate<sup>11</sup>, molybdate<sup>12</sup>, vanadate<sup>13</sup> and tungstate<sup>14</sup> phosphors or their mixed phosphors are chosen as the host material. Most of these phosphors give self-activated luminescence due to ligand-to-metal charge transfer (LMCT). The LMCT band is constituted by the transfer of charge from the filled electronic orbital of the ligand ion to the partially filled d sub-shell of the metal ion. The luminescence of these host phosphors can be tuned by doping rare-earth elements and transition metals. Rare-earth ( $\text{Re}^{3+}$ ) ions have an emission band under the 5d–4f transition that are strongly influenced by the crystal field of the host matrix, because the 5d orbital is very sensitive to the surrounding chemical environment. This causes the emission band of  $\text{Re}^{3+}$  ions to be weak in many hosts. In  $\text{Re}^{3+}$  ions, their forbidden intra f  $\rightarrow$  f transition is partially allowed due to the crystal field effect.<sup>15</sup> These intra f levels are intermediate energy levels in the bandgap whose transition results in sharp emission peaks. The phosphor must be chemically and thermally stable as these results in reduction of defect centers in the host lattice thereby reducing the possibility of non-radiative transition. There are many other requirements like chemical and thermal stability for the selection of phosphor materials which are mentioned below.

### 1.4.1 Requirements of phosphor materials

There are several requirements for phosphor materials that depend on their applications. Phosphor materials should have many distinctive properties considering the luminescence application, such as small particle size, high crystallinity, homogeneous distribution of the activator ions, high thermal stability, high chemical stability, near-UV excitation, emission in the visible range, longer decay lifetime and high luminescent intensity. The essentials of the phosphor, which is required for most applications, have been pointed out as follows;

- The phosphor should absorb UV light and give very efficient emission in the blue or green or red region with a high color rendering index (CRI).
- The phosphor should have excellent emissivity as well as optimum trap depth to free charge carriers at room temperature.
- The excitation of the phosphor for the white-LED should be in the range of 380 nm to 450 nm<sup>16</sup>, and the excitation for the plasma display should be 147 nm and 173 nm.<sup>17</sup>
- The phosphor must be of good thermal stability to give sufficient brightness at high temperatures.

Phosphors must be designed to provide excellent emission and high quantum efficiency, which is achieved by the selection of appropriate activator doping in the host matrix. The high efficiency and high luminous intensity of any phosphor depend largely on the activators that are doped from the host at a low concentration ratio. Activators must be active and have the least distortion in the host lattice to maintain the stability of the phosphor. Metal molybdates 'AMoO<sub>4</sub>' (A=Ca<sup>2+</sup>, Sr<sup>2+</sup>, Ba<sup>2+</sup>, etc) are a suitable phosphor for luminescence as it possesses all the required properties compared to other phosphor materials.<sup>18</sup> We have used CaMoO<sub>4</sub> as the host matrix in our research work as it gives better luminescence than other molybdates which are discussed in the section below.

### 1.4.2 Comparative study of CaMoO<sub>4</sub> with other alkaline earth metal molybdates

The crystal structure of the AMoO<sub>4</sub> phosphor is a tetragonal phase which is composed of [AO<sub>8</sub>]<sup>6-</sup> dodecahedral clouds and [MoO<sub>4</sub>]<sup>2-</sup> tetrahedral clouds attached to a common vertex A—O—Mo.<sup>19</sup> The luminescence in the AMoO<sub>4</sub> phosphor is achieved by allowing the forbidden transition of [MoO<sub>4</sub>]<sup>2-</sup> ions. The allowed transition of [MoO<sub>4</sub>]<sup>2-</sup> is due to the crystal field effect of [AO<sub>8</sub>]<sup>6-</sup> clouds.<sup>20</sup> Thus the crystal field strength depends on the A<sup>2+</sup>

ion affecting the luminescence. Generally,  $A^{2+}$  ions are selected from  $Ca^{2+}$ ,  $Sr^{2+}$  and  $Ba^{2+}$  ions for good luminescence. Among these, the  $Ca^{2+}$  ion gives the most excellent luminescence because the electro-negativity of the  $Ca^{2+}$  ion is higher than that of the other ions, which reduces the bond length of Ca–O bonds in  $[CaO_8]^{6-}$  clouds.<sup>20</sup> As a result, the crystal field is more affected around  $[MoO_4]^{2-}$  ions, achieving excellent luminescence.

### 1.4.3 $CaMoO_4$ phosphor as a host

$CaMoO_4$  phosphors have attracted much attention among the molybdates in the research fraternity due to their excellent properties likes, excellent emissivity in the visible region with near-UV excitation, high thermal stability, high crystallinity, high chemical stability, prolonged decay lifetime, more evenly distributed activator ions, etc.<sup>18</sup> The crystalline structure of the  $CaMoO_4$  phosphor is a tetragonal phase with  $I4_1/a$  space group symmetry.<sup>21,22</sup> The structure of  $CaMoO_4$  is composed of  $CaO_8$  dodecahedral and  $MoO_4$  tetrahedral clouds joined by a common edge Ca–O–Mo bond, respectively, as shown in Fig. 1.4.

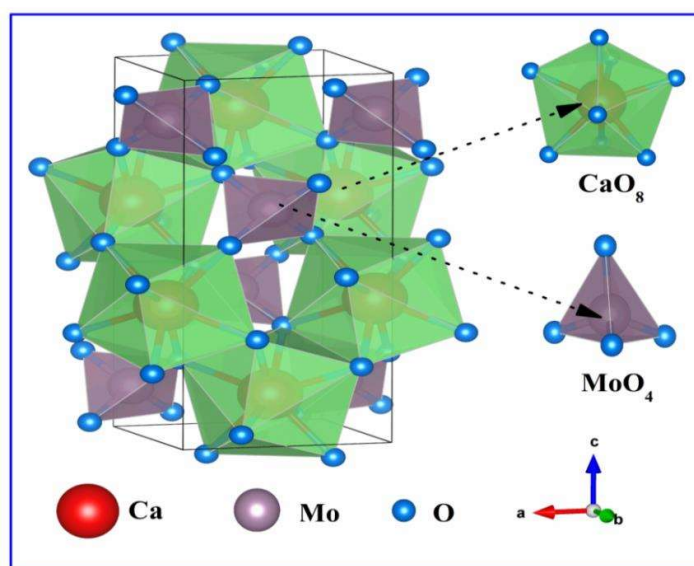


**Fig. 1.4** Crystal structure of  $CaMoO_4$  phosphor.

The  $\text{CaMoO}_4$  phosphor is an active luminescent which gives broad emission in the visible region under near-UV radiation. The UV radiation photons excite the  $\text{O}^{2-}$  electrons of the  $[\text{MoO}_4]^{2-}$  groups, leading to a transferring of charge between the filled  $\text{O}^{2-}$  orbit and partially filled  $\text{Mo}^{6+}$  orbit.<sup>22</sup> As a result, a broad emission band centered in green color is obtained. The excitation spectrum (PLE) is due to the ligand-to-metal charge transfer (LMCT) band, while the emission (PL) spectrum is attributed to the metal-to-ligand charge transfer (MLCT) band.<sup>23</sup> The PLE and PL spectrum of  $\text{CaMoO}_4$  phosphor are depicted in Fig. 1.5.

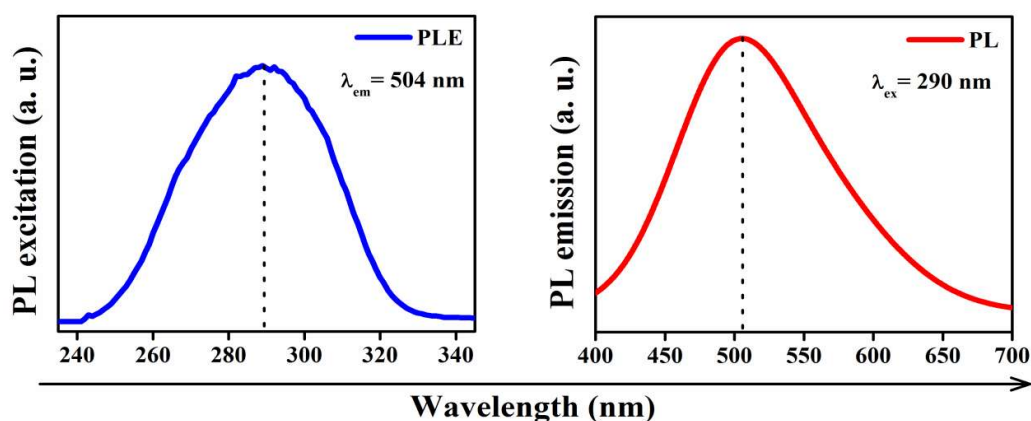


**Fig. 1.5** The PLE and PL spectrum of  $\text{CaMoO}_4$  phosphor.

### 1.5 Rare-earth ions

The groups consisting of Yttrium (Y) and Scandium (Sc) elements along with all the elements in the lanthanide (Ln) series are called rare-earth (Re) elements. All these elements are not found in pure form and out of these, cerium (Ce) is the 25<sup>th</sup> most abundant element on earth. The percentage of all these elements in the earth's crust is very low 0.3%, due to which they have been named rare-earth (Re) elements. Among the rare-earth (Re) elements, promethium (Pm) is a radioactive element obtained from the fission of the elements uranium (U) and thorium (Th). All these elements have been placed in the same family due to the similarity in their incredible chemical and optical properties. The

extraordinary optical properties of  $\text{Re}^{3+}$  ions have made them potential candidates for diverse applications over the past two decades in many fields such as lighting devices<sup>24-26</sup>, display devices<sup>27</sup>, forensic science<sup>28,29</sup>, bio-imaging<sup>30</sup>, sensing<sup>31</sup>, thermometry<sup>32,33</sup>, photocatalysis<sup>34,35</sup>, optical fibers<sup>36</sup>, and lasers<sup>37</sup>. The doping of  $\text{Re}^{3+}$  ions into the host matrix occurs as activation ions and co-activating ions that emit visible and near-infrared radiation under UV radiation excitation. The lanthanide ions ( $\text{Ln}^{3+}$ ) have an electronic configuration  $[\text{Xe}] 4f^n$  ( $n=0$  to 14) which is shielded by an environment of closed  $5s^2$  and  $5p^6$  shells. The  $\text{Ln}^{3+}$  electrons are arranged in various ways in the seven shells of 4f which is called degeneracy of  $[\text{Xe}] 4f^n$  configuration and each configuration is called micro state. The degeneracy of the  $4f^n$  configuration of  $\text{Ln}^{3+}$  ions can be partially and completely lifted by various perturbations. These disturbances are mainly spin-orbit coupling, crystal-field distortion, Zeeman Effect, and electron repulsion. The spin-orbit coupling is achieved due to the interaction of the electron's spin magnetic moment and the electron's orbital magnetic moment. The crystal-field effect is attributed to the interaction between the ligand's electrons and the 4f levels of the  $\text{Ln}^{3+}$  ion. The Zeeman Effect is caused by the splitting of energy levels in the presence of an external magnetic field. Electron repulsion arises from the electrostatic force between different electrons in the 4f shell. The state of each electron can be defined by a particular spectroscopic term, which refers to the three quantum numbers, the total spin quantum number (S), the total orbital angular momentum quantum number (L) and the total angular momentum quantum number (J). Where total angular momentum quantum number (J) is the resultant of the coupling of S and L quantum numbers. The spin-orbit coupling of the  $J^{\text{th}}$  level consists of  $2J+1$  degeneracy, and each  $J^{\text{th}}$  level is characterized by a  $^{2S+1}L_J$  spectroscopy term. The amount to which the  $2J+1$  degeneracy is eliminated depends on the symmetry class (cubic, tetragonal, hexagonal, octagonal, orthorhombic, trigonal, pentagonal, monoclinic and triclinic) and the symmetry

point group of the  $\text{Ln}^{3+}$  ions. The crystal field effect raises the  $2J+1$  degeneracy of the energy levels in the free ion even further and these levels are also known as the Stark levels or crystal field levels. The degeneracy of low-symmetry crystals (e.g. orthorhombic) is magnified by the crystal field effect, while the degeneracy of high-symmetry crystals (e.g. cubic) is magnified by the Zeeman Effect in the presence of an external magnetic field. The number of terms, multiplicity, number of levels, and ground level of all  $4f^n$  electronic configurations of  $\text{Ln}^{3+}$  ions are tabulated in Table 1.1.

**Table 1.1** Number of terms, multiplicity, number of levels, ground states and configurations for different Lanthanide ( $\text{Ln}^{3+}$ ) elements<sup>38</sup>

Lanthanide ( $\text{Ln}^{3+}$ ) ions	Configuration	No. of Terms	Multiplicity	No. of levels	Ground state
Lanthanum ( $\text{La}^{3+}$ )	$[\text{Xe}] 4f^0$	1	1	1	$^1\text{S}_0$
Cerium ( $\text{Ce}^{3+}$ )	$[\text{Xe}] 4f^1$	1	14	2	$^2\text{F}_{5/2}$
Praseodymium ( $\text{Pr}^{3+}$ )	$[\text{Xe}] 4f^2$	7	91	13	$^3\text{H}_4$
Neodymium ( $\text{Nd}^{3+}$ )	$[\text{Xe}] 4f^3$	17	364	41	$^4\text{I}_{9/2}$
Promethium ( $\text{Pm}^{3+}$ )	$[\text{Xe}] 4f^4$	47	1001	107	$^5\text{I}_4$
Samarium ( $\text{Sm}^{3+}$ )	$[\text{Xe}] 4f^5$	73	2002	198	$^6\text{H}_{5/2}$
Europium ( $\text{Eu}^{3+}$ )	$[\text{Xe}] 4f^6$	119	3003	295	$^7\text{F}_0$
Gadolinium ( $\text{Gd}^{3+}$ )	$[\text{Xe}] 4f^7$	119	3432	327	$^8\text{S}_{7/2}$
Terbium ( $\text{Tb}^{3+}$ )	$[\text{Xe}] 4f^8$	119	3003	295	$^7\text{F}_6$
Dysprosium ( $\text{Dy}^{3+}$ )	$[\text{Xe}] 4f^9$	73	2002	198	$^6\text{H}_{15/2}$
Holmium ( $\text{Ho}^{3+}$ )	$[\text{Xe}] 4f^{10}$	47	1001	107	$^5\text{I}_8$
Erbium ( $\text{Er}^{3+}$ )	$[\text{Xe}] 4f^{11}$	17	364	41	$^4\text{I}_{15/2}$
Thulium ( $\text{Tm}^{3+}$ )	$[\text{Xe}] 4f^{12}$	7	91	13	$^3\text{H}_6$
Ytterbium ( $\text{Yb}^{3+}$ )	$[\text{Xe}] 4f^{13}$	1	14	2	$^2\text{F}_{7/2}$
Lutetium ( $\text{Lu}^{3+}$ )	$[\text{Xe}] 4f^{14}$	1	1	1	$^1\text{S}_0$

### 1.5.1 Ln<sup>3+</sup> configuration transitions

Sir G. H. Dieke first gave a detailed summary of the configuration transitions of Ln<sup>3+</sup> ions and their energy levels in 1968.<sup>39,40</sup> They explained the energy levels of different Ln<sup>3+</sup> ions based on <sup>2S+1</sup>L<sub>J</sub> term values. The energy levels of the Ln<sup>3+</sup> ions are shown in Fig. 1.8. Basically, transitions of Ln<sup>3+</sup> ions are classified into three parts, which are 5d — 4f transitions, intra 4f — 4f transitions and charge transfer transitions, respectively.<sup>15</sup> These are mentioned one by one in the below section.

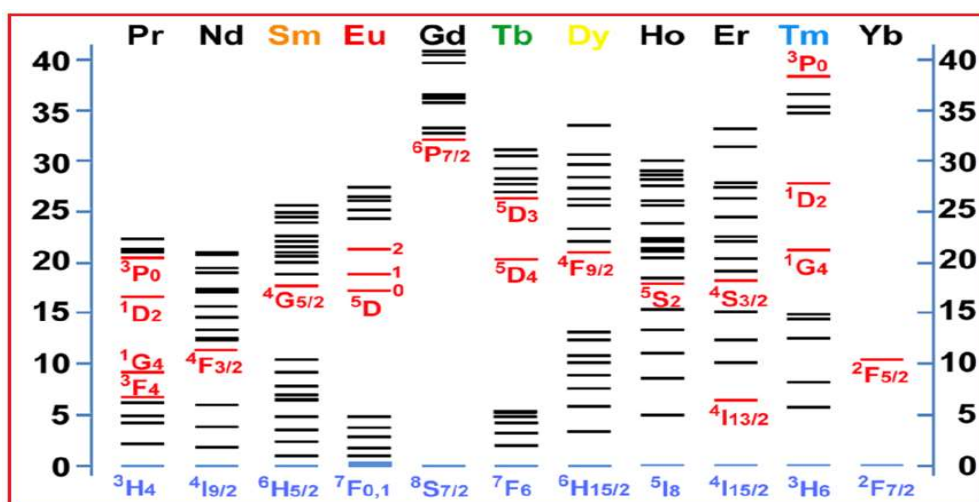


Fig. 1.6 Energy levels of different Ln<sup>3+</sup> ions.

#### 1.5.1.1 5d — 4f transitions

The 5d — 4f transitions are allowed because of the parity change, which obeys Laporte's selection rule. The selection rule shows whether an electronic transition is allowed or forbidden. The 5d orbital energy level splits under the influence of the crystal field of the host matrix, which forms a band from the overlap of many 5d orbital energy level partitions, resulting in a broad emission band. Hence the 4f — 5d transition can be easily tuned by

distortion in the crystalline structure. Some Re ions like  $\text{Sm}^{2+}$ ,  $\text{Ce}^{3+}$ ,  $\text{Eu}^{2+}$  etc give extensive emission due to the  $5d \rightarrow 4f$  transition.<sup>41-43</sup>

### **1.5.1.2 Intra 4f — 4f transitions**

The  $4f \rightarrow 4f$  transition occurs as a result of the intra electronic transition between different shells of the f orbital. Generally, the prominent electronic transitions of  $\text{Ln}^{3+}$  ions are sum-parity magnetic dipoles transition (MD) and odd-parity electric dipoles transition (ED). The  $\text{Ln}^{3+}$  ion interacts with the magnetic field vector of the magnetic dipole resulting in the MD transition; similarly, the interaction of the  $\text{Ln}^{3+}$  ion with the electric field vector of an electric dipole gives ED transition. Intra-ED transitions do not obey Laporte's selection rule due to forbidden transitions if the ground state and the excited state have the same symmetry as the inversion centre. Furthermore, when  $\text{Ln}^{3+}$  ions enter the host lattice, they are affected by the ligand region. This causes their 4f wave functions to overlap with higher configurations resulting in a coupling of electronic and vibrational states called the vibronic state. The Laporte rule relaxes the vibronic state, allowing the ED transition to be partially induced. Therefore, ED transitions are called forced or induced ED transitions. This forced transition is very sensitive to the surrounding environment of  $\text{Ln}^{3+}$  ions. Furthermore, the MD transition permits parity, making the MD transition much less sensitive to the chemical environment around the  $\text{Ln}^{3+}$  ion. The intensity of MD transition is weaker than that of ED transition. The MD transitions obey the selection rules from the 'Judd-Ofelt' principle,  $\Delta S = 0$ ,  $\Delta L = 0$ , and  $\Delta J = 0, \pm 1$  while the forced ED transition follows  $\Delta S = 0$ ,  $\Delta L \leq 6$  (as  $\Delta L = 2, 4, 6$ ), and  $\Delta J \leq 6$  (as  $\Delta J = 2, 4, 6$ ). Transitions of the higher order, such as the electric quadrupole transition, have a very low intensity and are rarely seen in the spectrum. The 4f orbital is shielded from the 5s and 5p orbital so that it does not split its orbital energy levels

and doesn't form a broad band. As a result, a narrow emission is obtained due to 4f—4f transition.

### 1.5.1.3 Charge transfer transitions

The transfer of electrons from the excited state of an ion to the excited state of another ion of the same compound is called a charge transfer transition.  $\text{Ln}^{3+}$  corresponding charge transfer transitions are mainly possible between  $\text{Ln}^{3+}$  ions from the ligand of the same compound, between two  $\text{Ln}^{3+}$  ions, or between  $\text{Ln}^{3+}$  ions from the central cation of the host matrix. These transitions are allowed by Laporte's selection rule. We can understand this by taking the example of  $\text{Dy}^{3+}$  doped  $\text{CaMoO}_4$ , in which a charge transfer band centered at 290 nm is obtained corresponding to the  $\text{O}^{2-} \rightarrow \text{Dy}^{3+}$  transition.<sup>21</sup> This transition is a ligand-to-metal charge transfer transition resulting from the transfer of charge from a filled p orbital of the  $\text{O}^{2-}$  ion to a partially filled f orbital of the  $\text{Dy}^{3+}$  ion.

### 1.6 Rare-earth ( $\text{Re}^{3+}$ ) ions used in research work

We have used 4 different types of trivalent  $\text{Re}^{3+}$  ions in our research work which are Europium ion ( $\text{Eu}^{3+}$ ), Dysprosium ion ( $\text{Dy}^{3+}$ ), Samarium ion ( $\text{Sm}^{3+}$ ), and Terbium ion ( $\text{Tb}^{3+}$ ). The  $\text{CaMoO}_4$  host is already doped with many lanthanide ions, of which we have selected these four on the basis of their emission color which is important for white light LEDs. White light can be obtained by the combination of red, green, and blue light. The prominent emission of  $\text{Eu}^{3+}$  and  $\text{Sm}^{3+}$  ions lie in the red region and that of  $\text{Tb}^{3+}$  ion lies in the green region. Therefore,  $\text{Eu}^{3+}$  and  $\text{Sm}^{3+}$  ions are used as a red emission source and  $\text{Tb}^{3+}$  ions as a green emission source, which can be deposited on a blue chip to produce white light under the excitation of the blue chip. While  $\text{Dy}^{3+}$  ion has two prominent emissions, the combination of which results in the near-white light region, due to which  $\text{Dy}^{3+}$  ion has

also been chosen for doping in his research works. All these are explained one by one in the below sections.

### 1.6.1 Europium ( $\text{Eu}^{3+}$ ) ion

The europium ion ( $\text{Eu}^{3+}$ ) has the electronic configuration  $[\text{Xe}] 4f^6$  and has 6 electrons in its outermost f orbital. The intense luminescence is achieved in  $\text{Eu}^{3+}$  doped compounds due to the charge transfer of  $\text{Eu}^{3+}$  ion from excited state  ${}^5\text{D}_0$  to ground state  ${}^7\text{f}_j$  ( $J=0$  to  $6$ ). The principle of the Judd–Ofelt theory explicitly forbids this  ${}^5\text{D}_0 \rightarrow {}^7\text{F}_0$  transition, since the presence of this transition suggests that the  $\text{Eu}^{3+}$  ion is located in the  $\text{C}_{nv}$ ,  $\text{C}_n$ , or  $\text{C}_s$  site symmetry of the lattice. Generally, the strength of a magnetic dipole (MD) transition ( ${}^5\text{D}_0 \rightarrow {}^7\text{F}_1$ ) is unaffected by the surroundings of the  $\text{Eu}^{3+}$  ion. The  ${}^5\text{D}_0 \rightarrow {}^7\text{F}_1$  transition is more intense in substances with centre symmetric crystal structures, due to the effect of  ${}^7\text{F}_1$  crystal field splitting on the  ${}^5\text{D}_0 \rightarrow {}^7\text{F}_1$  transition<sup>44</sup>. Furthermore, the electric dipole transition  ${}^5\text{D}_0 \rightarrow {}^7\text{F}_2$  is known as a "hypersensitive transition" because the environment surrounding the  $\text{Eu}^{3+}$  ion has a substantial effect on its intensity. The asymmetry around the  $\text{Eu}^{3+}$  ion is often measured by the strength of the  ${}^5\text{D}_0 \rightarrow {}^7\text{F}_2$  hypersensitive transition. If the intensity of the  ${}^5\text{D}_0 \rightarrow {}^7\text{F}_2$  transition is at its maximum, the  $\text{Eu}^{3+}$  ion will certainly occupy the lower symmetry in the host lattice. The  ${}^5\text{D}_0 \rightarrow {}^7\text{F}_2$  transition results in the characteristic red fluorescence of the  $\text{Eu}^{3+}$  ion. The Judd–Ofelt principle states that the  ${}^5\text{D}_0 \rightarrow {}^7\text{F}_3$  transition is forbidden, so it is significantly weaker. The transition from  ${}^5\text{D}_0$  to  ${}^7\text{F}_4$  is another electric dipole transition. The  ${}^5\text{D}_0 \rightarrow {}^7\text{F}_4$  transitions in the compounds show the predominance of  $\text{D}_{4d}$  symmetry. Additionally,  ${}^5\text{D}_0 \rightarrow {}^7\text{F}_5$  and  ${}^5\text{D}_0 \rightarrow {}^7\text{F}_6$  are two more transitions that are rarely observed because they occur above 800 nm, where most spectrophotometer detectors have poor sensitivity. The luminescence of the  $\text{Eu}^{3+}$  ion can also come from the  ${}^5\text{D}_J$  ( $J=0, 1, 2$ ) levels in some inorganic hosts. The absorption spectra

of the  $\text{Eu}^{3+}$  ion yield peaks correspond to the  ${}^7\text{F}_0 \rightarrow {}^5\text{D}_J$  ( $J = 0, 1, 2$ ) transition. The  $\text{Eu}^{3+}$  doped compounds are being researched for use in various fields, such as red phosphors for lighting and displays, luminous markers in biology, etc.<sup>45-47</sup> The  $\text{Eu}^{3+}$  doped phosphors can also be used in optical thermometry because the  ${}^5\text{D}_0$  and  ${}^5\text{D}_1$  energy levels of the  $\text{Eu}^{3+}$  ion are thermally coupled.<sup>48</sup> Additionally, the local symmetry around the rare-earth ion can also be investigated using the  $\text{Eu}^{3+}$  ion. Thus, the  $\text{Eu}^{3+}$  ion is useful in various applications due to its potentiating properties.

### 1.6.2 Dysprosium ( $\text{Dy}^{3+}$ ) ion

The electronic configuration of dysprosium ion ( $\text{Dy}^{3+}$ )  $[\text{Xe}] 4\text{f}^9$  is that it has 9 electrons in its outermost f shell. The excitation spectrum of the  $\text{Dy}^{3+}$  ion consists of sharp peaks in the near-UV and visible region due to electronic transitions from the ground level  ${}^6\text{H}_{15/2}$  to the excited states  ${}^6\text{P}_{3/2}$ ,  ${}^6\text{P}_{7/2}$ ,  ${}^4\text{I}_{11/2}$ ,  ${}^4\text{I}_{13/2}$ ,  ${}^4\text{G}_{11/2}$ ,  ${}^4\text{I}_{15/2}$  and  ${}^4\text{F}_{9/2}$ . The emission spectrum of the  $\text{Dy}^{3+}$  ion consists of blue, yellow, and red intense peaks observed corresponding to the transition from excited state  ${}^4\text{F}_{9/2}$  to ground states  ${}^6\text{H}_J$  ( $J = 7/2, 9/2, 11/2, 13/2, \text{ and } 15/2$ ).<sup>49</sup> Additionally, one more emission peak in  $\text{Dy}^{3+}$  ions is observed in the blue region corresponding to  ${}^4\text{I}_{15/2} \rightarrow {}^6\text{H}_{15/2}$  transition. In the emission spectrum, the  ${}^4\text{F}_{9/2} \rightarrow {}^6\text{H}_{13/2}$  transition is a forced ED transition that is highly sensitive to the chemical environment around the  $\text{Dy}^{3+}$  ions, whereas the  ${}^4\text{F}_{9/2} \rightarrow {}^6\text{H}_{13/2}$  transition is an MD transition that is not affected by the surrounding environment. We know that white light can be obtained from a combination of blue, green and red luminescence. The  $\text{Dy}^{3+}$  ion is a better activator ion for white-light emission applications, as its sharp emission occurs mainly in the blue, greenish-yellow and red regions. Furthermore, the  $\text{Dy}^{3+}$  emission transitions  ${}^4\text{F}_{9/2} \rightarrow {}^6\text{H}_{15/2}$  and  ${}^4\text{I}_{15/2} \rightarrow {}^6\text{H}_{15/2}$  are thermal pair transitions.<sup>50</sup> Therefore, if the intensity of one of these emissions increases with an increase in temperature, then the intensity of the other

decreases, and whose intensity ratio versus temperature graph follows an exponential sequence. Therefore,  $\text{Dy}^{3+}$  doped various phosphors can also be used in optical thermometry applications.

### 1.6.3 Samarium ( $\text{Sm}^{3+}$ ) ion

The electronic configuration of the samarium ion ( $\text{Sm}^{3+}$ ) is  $[\text{Xe}] 4f^6$  so it has five electrons in its outermost f shell. The excitation spectrum of the  $\text{Sm}^{3+}$  ion is obtained sharp peaks in the near-UV and visible region, which attributed to the electronic transition from the ground level  $^4\text{H}_{5/2}$  to the excited states  $^4\text{L}_{17/2}$ ,  $^6\text{K}_{11/2}$ ,  $^4\text{F}_{7/2}$ ,  $^6\text{P}_{5/2}$ ,  $^4\text{I}_{13/2}$ ,  $^4\text{I}_{11/2}$  and  $^4\text{I}_{9/2}$ . Among this excitation, the  $^4\text{H}_{5/2} \rightarrow ^4\text{F}_{7/2}$  transition is the most intense. Some sharp peaks are observed in the orange to the red visible region in the emission spectrum of the  $\text{Sm}^{3+}$  ion, which results from the electronic transitions  $^4\text{G}_{5/2} \rightarrow ^6\text{H}_J$  ( $J=5/2, 7/2, 9/2, 11/2, 13/2$ ).<sup>51</sup> The emission transition  $^4\text{G}_{5/2} \rightarrow ^6\text{H}_{5/2}$  is an MD transition. Whereas  $^4\text{G}_{5/2} \rightarrow ^6\text{H}_{9/2}$  is an ED transition with  $\Delta J=2$  so it is hypersensitive. Additionally, the  $^4\text{G}_{5/2} \rightarrow ^6\text{H}_{7/2}$  transition is neither a complete MD nor a complete ED transition. The  $\text{Sm}^{3+}$  ion is a better activation ion as a good red emitter for lighting and display device applications.

### 1.6.4 Terbium ( $\text{Tb}^{3+}$ ) ion

The electronic configuration of the terbium ion ( $\text{Tb}^{3+}$ ) is  $[\text{Xe}] 4f^8$  so it has 8 electrons in its outermost f shell. The emission spectra of the  $\text{Tb}^{3+}$  ion consist of four prominent peaks in the visible region, which correspond to transitions  $^5\text{D}_4 \rightarrow ^7\text{F}_J$  ( $J=6, 5, 4, 3$ ).<sup>52</sup> The  $\text{Tb}^{3+}$  transition  $^5\text{D}_4 \rightarrow ^7\text{F}_6$  obtained at the blue region is an ED transition and the  $\text{Tb}^{3+}$  transition  $^5\text{D}_4 \rightarrow ^7\text{F}_5$  obtained at the green region is an MD transition. The MD transition of  $\text{Tb}^{3+}$  ions is less sensitive to the surrounding chemical environment of  $\text{Tb}^{3+}$  ions, whereas the ED transition is sensitive but not hyper-sensitive. The intensity of electric dipole transition depends on both the nature of ligand and its sensitivity to the surrounding chemical

environment. Due to which the ED transition in  $Tb^{3+}$  ions is not known to be affected much by the crystal region of the ligand ion. As a result, the MD transition is more intense than the ED transition. Hence, the  $Tb^{3+}$  doped phosphors emit green light due to the strong  $^5D_4 \rightarrow ^7F_5$  transition. The  $Tb^{3+}$  ion is a better activation ion as a good green emitter for lighting and display device applications.

The Jablonski diagrams of these  $Re^{3+}$  ions ( $Eu^{3+}$ ,  $Dy^{3+}$ ,  $Sm^{3+}$ , and  $Tb^{3+}$ ) and their excitation-emission transitions are shown below in Fig. 1.7.

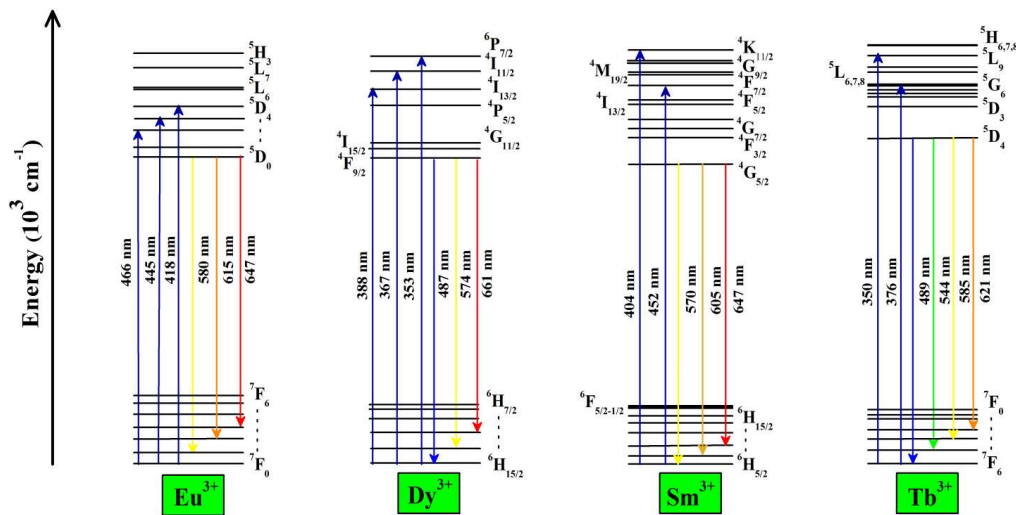
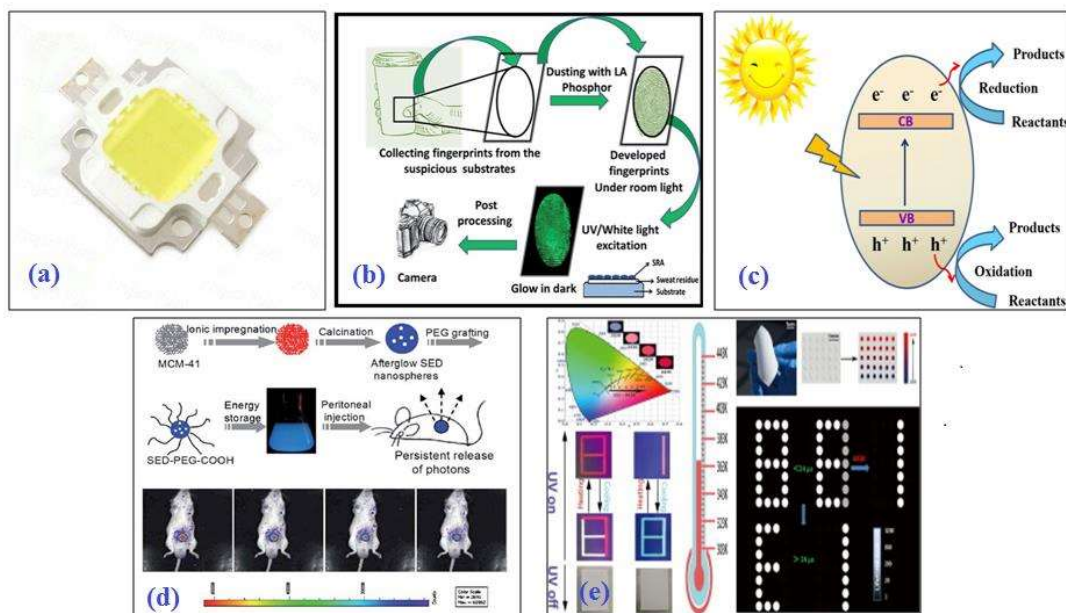


Fig. 1.7 Jablonski diagram, excitation and emission transitions of  $Eu^{3+}$ ,  $Dy^{3+}$ ,  $Sm^{3+}$  and  $Tb^{3+}$  ion.

### 1.7 Application of rare-earth doped phosphor materials

Phosphor materials have revolutionized scientific and technological progress with their excellent optical properties, which are exhibited by these phosphors upon the incorporation of activator ions into the host lattice. Due to the light-emitting properties of phosphor materials, it is used in many applications in various fields, such as optoelectronics<sup>24–26</sup> (white light-emitting diodes (wLEDs) and display devices), sensing field<sup>31–33</sup> (temperature

and UV sensing), bio-medical science<sup>30</sup> (bio-imaging), forensic science<sup>28,29</sup> (latent fingerprint detection), photo-catalysis<sup>34,35</sup> and so on other fields.



**Fig. 1.8** (a) White light emitting diode chip, (b) Phosphor use for fingerprint detection technique<sup>53</sup>, (c) As a photocatalysis<sup>54</sup>, (d) Bio-imaging application<sup>55</sup> and (e) Optical thermometry application<sup>56</sup>.

White light emitting diode (wLED), one of the major uses of phosphor materials, has made significant inroads in the lighting industry. Scientists and researchers envisage many exciting uses for wLEDs, such as liquid crystal displays, phototherapy, and indoor farming, along with increasing their efficacy and stability of them. We have discussed the white light-emitting application of phosphor materials in our research work. The commercial wLEDs currently in use and their drawbacks are discussed in detail. Furthermore, the parameters required to overcome those deficiencies are discussed.

Phosphor-formed wLEDs have appeared as a potential replacement for next-generation conventional light sources. wLEDs offer many advantages over conventional light sources, among which are low power consumption (less than 8.5 W), high luminous efficiency

(greater than  $100 \text{ lm/W}$ ), a long operating lifetime (50,000 hours), great brightness (800 more than), flexibility, and environmental friendliness.<sup>57</sup> Advantages of wLEDs over other traditional sources are depicted in Fig. 1.9. Nowadays, LEDs are used as essential components in a wide variety of applications, including display devices, medical applications, outdoor and indoor lighting, workplaces and road signal illumination.

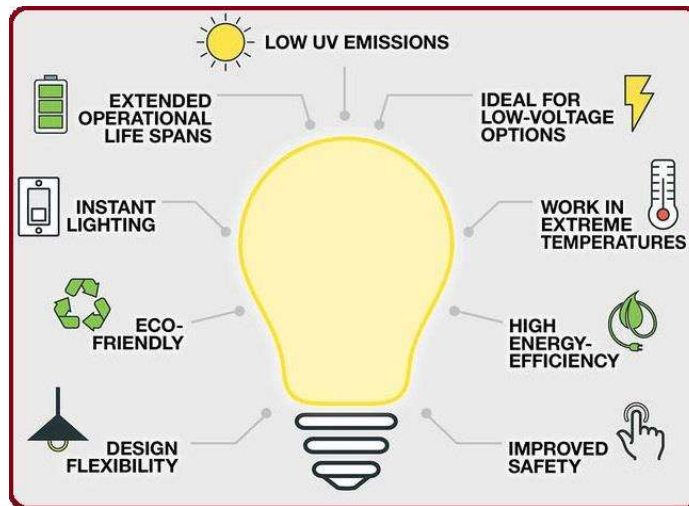


**Fig. 1.9** Advantages of wLEDs over other traditional light sources.

The first wLED was successfully fabricated by Y. Shimizu and his group members in Nichia lab by the coating of  $\text{Ce}^{3+}$  doped YAG yellow phosphor on an InGaN chip.<sup>58</sup> Farther, Isamu Akasaki, along with two other colleagues, contributed to improving the luminous efficiency of wLEDs from  $25 \text{ lm/W}$  to  $200 \text{ lm/W}$  by the construction of high-efficiency blue-emitting LEDs, which earned them the Nobel Prize. Thereby, the light generated by the blue LED chip excites the yellow phosphor, and bluish-white light is obtained by the adjustment of yellow light and blue light. The fabrication and emission spectrum of commercial wLED are represented in Fig. 1.10.

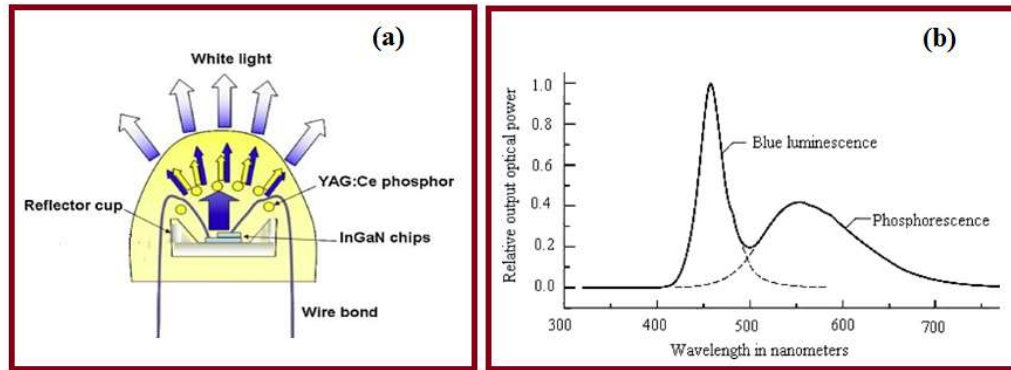


**Fig. 1.10 (a)** Fabrication of commercial wLED<sup>59</sup> and **(b)** Luminescence spectrum of commercial wLED<sup>59</sup>.

High luminous efficiency has been achieved in commercial wLED to date, but it still has many shortcomings. As we know that to get proper white light there should be an equal contribution of blue, yellow, and red-emitting, but commercial wLED lack red emitting which results in its color rendering index (CRI) being less than 75 and correlated color temperature (CCT) is greater than 5000 K.<sup>60</sup> The high CCT value is not comfortable for the human eye, which is the main drawback of commercial wLEDs. Basic information about the color emitted by any phosphor is obtained from the chromaticity parameters, which are evaluated from its PL emission spectrum. In many industrial sectors, wLEDs are made by combining three different LEDs of blue, yellow and red. The white color obtained with this technique has several significant drawbacks such as color ratio coordination, color re-absorption, and efficiency of radiation.<sup>61</sup> Therefore, a better approach is to obtain high luminous efficiency LEDs by reducing the drawbacks of wLEDs fabricated by depositing the color phosphor on top of the blue-chip. Moreover, the  $\text{Ce}^{3+}$  doped YAG yellow phosphor used in commercial wLEDs has low thermal stability, losing about 50% of its emission intensity at 150 °C compared to room temperature.<sup>62</sup> Thus, to obtain excellent white light emission, color phosphors with better chromaticity parameters should be

thermally/chemically stable. We have mentioned those chromaticity parameters one by one in the section below.

## **1.8 Chromaticity parameters**

### **1.8.1 Commission Internationale de l'Éclairage (CIE) coordinates**

The International Commission on Illumination often called the “Commission Internationale de l'Éclairage” (CIE), developed the CIE color model which is known as the CIE 1931 XYZ color space.<sup>63</sup> This model is a mapping method that uses tri-stimulus (a combination of red, green, and blue color values) that is shown in 3 dimensions. When these variables are added together, they can recreate any hue that the human eye can detect. The CIE standard is intended to precisely represent every hue that the human eye can detect. CIE coordinates ( $x$ ,  $y$ , and  $z$ ) are represented by three tri-stimulus values  $X$ ,  $Y$ ,  $Z$ , which represent the values corresponding to red, green, and blue.<sup>63</sup>

$$x = \frac{X}{X+Y+Z}, y = \frac{Y}{X+Y+Z} \text{ and } z = \frac{Z}{X+Y+Z} \quad 1.5$$

The sum of  $x$ ,  $y$ , and  $z$  in CIE coordinates is 1, so the value of  $z$  can be determined from the value of  $x$  and  $y$  and the CIE coordinates can be represented by  $(x, y)$ . According to the National Television Standards Committee (NTSC), the CIE coordinate for perfect white emitting color is (0.33, 0.33), which is derived from an equal ratio of the RGB tricolours.

### **1.8.2 Color rendering index (CRI)**

The color rendering index (CRI) is a unit-less index classified on a scale of 0 to 100 that measures the ability of a light source to reproduce the colors of a variety of objects in contrast to sunlight. The CRI of sunlight is 100. A higher CRI value indicates the accuracy of the colors. CRI was developed in response to the fact that the same object appears differently under different light spectrum distributions. CRI is determined as the difference

in chromaticity of eight CIE standard color samples when an object is lit by a single light source and a reference light with the same associated color temperature. Therefore, the smaller the average differences in chromaticity, the higher the CRI value.

### **1.8.3 Correlated color temperature (CCT)**

A method for calculating correlated color temperature (CCT), which is one of a light source's apparent color characteristics and relates to a black body locus, is to measure the temperature of the light on an iso-temperature line on the chromaticity chart. The measurement is made in absolute temperature Kelvin (K). It should not be confused with the heat that any light source emits. The CIE 1931 chromaticity diagram shows the route that the color of an incandescent black body would travel when temperature shifted or changed. This path is known as the "black body locus." When the temperature is high, it transitions from reddish at low temperatures to orange, yellowish-white, white, and blue-white. The CCTs exceeding 6,000 K are referred to as cool colors (bluish-white), whereas lower color temperatures (1,500–3,500 K) are referred to as warm colors.<sup>25</sup> Since these hues do not lie inside the black body locus, the color temperature should not be used for green or purple lights. For applications like lighting, photography, videography, and other industries that utilize lighting, color temperature is a crucial consideration. The CCT for the CIE 1931 chromaticity model is calculated by the following formula<sup>64</sup>;

$$CCT = 437n^3 + 3601n^2 + 6861n + 5524.31 \quad 1.6$$

where  $n$  is calculated by  $(x-0.3320)/(0.1858-y)$  for the CIE coordinates  $(x, y)$  of a phosphor, and the CCT value for neutral white light is in the range from 4000 K to 5000 K.

### **1.8.4 Color purity (CP)**

The term color purity (CP) refers to the amount of specific brightness of a monochromatic color of radiation emitted by a light source, expressed as a percentage. Its value is 100 for ideal monochromatic radiation (as a LASER source) and 0 for ideal multi-chromatic source. The color purity is evaluated in the CIE chromaticity diagram by the following expression<sup>37</sup>;

$$CP \text{ (in \%)} = \sqrt{\frac{(x-x_o)^2 + (y-y_o)^2}{(x_p-x_o)^2 + (y_p-y_o)^2}} * 100 \quad 1.7$$

where  $(x_o, y_o)$  is the white illuminant point in the 1931 CIE standard chromaticity diagram and  $(x, y)$  is the CIE coordinates of the phosphor. In addition,  $(x_p, y_p)$  is the peripheral coordinate in a chromaticity diagram obtained by extending the line joining the  $(x, y)$  coordinate to the white illuminant coordinate. The minimum value of color purity represents the quality of white light.

### **1.8.5 Luminous efficiency**

Luminous efficacy is a measure of a light source's performance that determines how much energy is transformed into light and how well the light produced is perceived by the human eye. It is calculated as the ratio of input power to total luminous flux output. The maximum luminous efficacy of a light source that is theoretically achievable is 683 lm/W.<sup>65</sup>

A better wLED can be made by controlling these chromaticity parameters as well as other constraints such as stability at high temperatures, a supportive environment for the synthesis process, the need for large investments and their practical applicability, etc.

### 1.9 Inspirations for thesis

The thesis work is directed at the luminescence study of rare-earth ( $\text{Re}^{3+}$ ) ion-doped  $\text{CaMoO}_4$  for the applications of white-LED. Commercial wLEDs have a highly correlated color temperature ( $\text{CCT} > 5000 \text{ K}$ ) and limited color rendering index ( $\text{CRI} < 75$ ) due to the lack of red emission, and the thermal stability of the deposited yellow phosphor is very low. Therefore, commercial wLEDs have several shortcomings whose improvement is the motivation for our work. Better wLEDs can be achieved either by depositing thermally stable green and yellow phosphors excited by blue chip emission on top of blue chip InGaN or by improving single component phosphors giving emission in the near white light region. Many researchers have reported red and green phosphors made by low thermal/chemical stability and difficult synthesis methods for the development of light-emitting applications, which inspired us to develop excellent red/green emission phosphors with eco-friendly, high thermal/chemical stability which is prepared by easy synthesis process. Additionally, we have found from literature surveys that the emission intensity of  $\text{Re}^{3+}$  ions can be improved with the doping of transition metal ions ( $\text{Zn}^{2+}$ ,  $\text{Mn}^{2+}$ ) and bismuth ions ( $\text{Bi}^{3+}$ ). These ions move easily into the host lattice sites and increase the asymmetry, resulting in a change in the crystal field around the  $\text{Re}^{3+}$  ions. The altered crystal field greatly affects the forced electric dipole transitions of the  $\text{Re}^{3+}$  ion, thereby improving the emission intensity. Moreover, transition metal ions and bismuth ions doping leads to a decrease in host lattice defects and an improvement in crystallinity. The absorption energy absorbed by the phosphor is spent on exciting the electrons of the ligand, instead of being lost in the defect centers, which increases the population of the excited electrons, and consequently increases the intensity of the emission. Thus the luminescence intensity of  $\text{Re}^{3+}$  ion can be enhanced by doping transition metal ions and bismuth ions in  $\text{Re}^{3+}$  doped phosphor. We have investigated optical properties caused by co-doping of  $\text{Mn}^{2+}$  in  $\text{Eu}^{3+}$  doped  $\text{CaMoO}_4$

red phosphor and optical properties caused by co-doping of  $\text{Bi}^{3+}$  ion in  $\text{Tb}^{3+}$  doped  $\text{CaMoO}_4$  green phosphor. In addition, we have also investigated the thermal stability of  $\text{Bi}^{3+}$  co-doped  $\text{Tb}^{3+}$  doped  $\text{CaMoO}_4$  phosphors.

Many researchers have developed  $\text{Dy}^{3+}$  doped other phosphors as white light emitters to get rid of the difficult technique of coating the phosphor over the blue chip. The  $\text{Dy}^{3+}$  has two major emission peaks in the blue and yellow regions, which combine to produce white light. But due to the lack of red emission, its CIE coordinates are not at the white light point and its CCT value is more than 5000 K. We have learned from literature surveys that by co-doping appropriate  $\text{Re}^{3+}$  ions, energy can be transferred from  $\text{Dy}^{3+}$  to co-doped  $\text{Re}^{3+}$ . Thereby, the emission of  $\text{Dy}^{3+}$  and co-doped  $\text{Re}^{3+}$  ions can be controlled by the  $\text{Re}^{3+}$  ion concentration and excellent white light can be obtained. Red-emitting  $\text{Re}^{3+}$  ions (such as  $\text{Sm}^{3+}$ ) can be doped to improve the CIE and CCT values. Thus, cost-effective single-component superior white light emitters can be easily fabricated. We have controlled the CIE coordinates and CCT temperature of the emitted white light of  $\text{Dy}^{3+}$  doped  $\text{CaMoO}_4$  by co-doping  $\text{Zn}^{2+}$  and  $\text{Sm}^{3+}$  ions and also investigated its thermal stability. We have explained the energy transfer mechanism between  $\text{Dy}^{3+}$  to  $\text{Sm}^{3+}$  in our published papers and converted cold white light to neutral white light.

An excellent host for  $\text{Re}^{3+}$  ions is the  $\text{CaMoO}_4$  phosphor because it enables effective and simultaneous energy transfer from the host LMCT band to the energy levels of the doped  $\text{Re}^{3+}$  ions. As a result, intense emission of  $\text{Re}^{3+}$  ions is obtained, in which further improvement can be achieved by co-doping transition metals and bismuth ions, and the emitted color can be tuned by co-doping another  $\text{Re}^{3+}$  ion. Thus,  $\text{Zn}^{2+}$  or  $\text{Sm}^{3+}$  co-doped  $\text{Dy}^{3+}$  doped  $\text{CaMoO}_4$  is a cost-effective synthetic and thermally/chemically stable phosphor with excellent emissivity, making it a superior candidate for wLED applications.